Supplemental Figure 1

A

Chr.	*idd*	Marker	Δ (cM)[a]	N6F2 Tssp°	N10F2 Tssp°	N13F2 Tssp°	N13F2 WT
1	*idd5*	D1Mcq136	0.1	NOD	NOD	NOD	NOD
	idd26	D1Mit212	1	NOD	NOD	NOD	NOD
2	*idd13*	D2Mit17	2	NOD (3/6) NOD/B6 (2/6)	NOD	NOD	NOD
3	*idd3*	D3Mit151	0.7	NOD	NOD	NOD	NOD
	idd17	D3Mit100	6.8	NOD	NOD	NOD	NOD
	idd10	D3Mit12	0.7	NOD	NOD	NOD	NOD
	idd18	D3Mit284	1.9	NOD	NOD	NOD	NOD
4	*idd11/25*	D4Mit203	1.9	NOD	NOD	NOD	NOD
	idd9	D4Mit15	0	NOD (5/6) NOD/B6 (1/6)	NOD	NOD	NOD
5	*idd15*	D5Mit48	0	NOD	NOD	NOD	NOD
6	*idd20*	D6Mit8	1	NOD	NOD	NOD	NOD
	idd19	D6Mit135	1.8	NOD	NOD	NOD	NOD
	idd6	D6Mit15	1	NOD	NOD	NOD	NOD
7	*idd7*	D7Mit328	1.3	NOD	NOD	NOD	NOD
	idd27	D7Mit235	2.9	NOD	NOD	NOD	NOD
8	*idd22*	D8Mit238	2.9	NOD	NOD	NOD	NOD
9	*idd2*	D9Mit205	3	NOD	NOD	NOD	NOD
11	*idd4*	D11Mit339	12	NOD	NOD	NOD	NOD
13	*idd14*	D13Mit61	0	NOD	NOD	NOD	NOD
14	*idd8*	D14Mit110	0	NOD (5/6) B6 (1/6)	NOD	NOD	NOD
	idd12	D14Mit222	5.5	NOD (5/6) B6 (1/6)	NOD	NOD	NOD
17	*idd23*	D17Mit113	1.5	NOD	NOD	NOD	NOD
	idd1	FACS MHC II		NOD	NOD	NOD	NOD
	idd16	D17Mit28	0.4	NOD	NOD	NOD	NOD
18	*idd21*	D18Mit74	0.5	NOD	NOD	NOD	NOD

[a] Δ cM refers to the distance in cM between the position of a given *idd* locus and that of the relevant marker used for analysis. Genetic position were obtained from *Mouse Genome Informatics* database.

B

Chromosome 13					
Marker	Position (cM)[a]	Status			
		N6F2 Tssp°	N10F2 Tssp°	N13F2 Tssp°	N13F2 WT
D13 Mit 205	5	129[b]	**NOD**	**NOD**	**NOD**
D13 Mit 80	8	129	**NOD**	**NOD**	**NOD**
D13 Mit 17	8	129	129	**NOD**	**NOD**
D13 Mit 57	9	129	129	**NOD**	**NOD**
D13 Mit 218	9	129	129	**NOD**	**NOD**
D13 Mit 271	9	129	129	**NOD**	**NOD**
Prss16	10				
D13 Mit 163	11	129	129	129	**NOD**
D13 Mit 117	19	129	**NOD**/129	129	**NOD**
D13 Mit 177	21	129	**NOD**/129	129	**NOD**
D13 Mit 61	22	**NOD**	**NOD**	**NOD**	**NOD**
Idd14	22				

[a] Genetic position obtained from Mouse Genome Informatics database.
[b] 129/Sv strain.

Supplemental Figure 1. Resistance of Tssp° NOD mice to insulitis and diabetes is unlikely to rely on genetic alteration of insulin-dependent diabetes (*idd)* intervals associated with disease susceptibility.
(**A**) Microsatellite marker analysis of all known *idd* loci in Tssp° and WT NOD littermates at the N6, N10 and N13 backcross generation. At the N6 backcross generation all mice used in Figure 1A were analyzed. In case of heterogeneity, the number of mice with the NOD, B6 or NOD/B6 alleles are indicated in parenthesis. At the N10 and N13 backcross generation males and females mice used to generate the corresponding WT and Tssp° line were analyzed. (**B**) Microsatellite marker analysis of chromosome 13 (5 – 22 cM region) from N6F2 Tssp°, N10F2 Tssp°, N13F2 Tssp° and N13F2 WT NOD mice. Microsatellite markers that are polymorphic between NOD, C57BL/6 and 129 were used for genetic characterization.

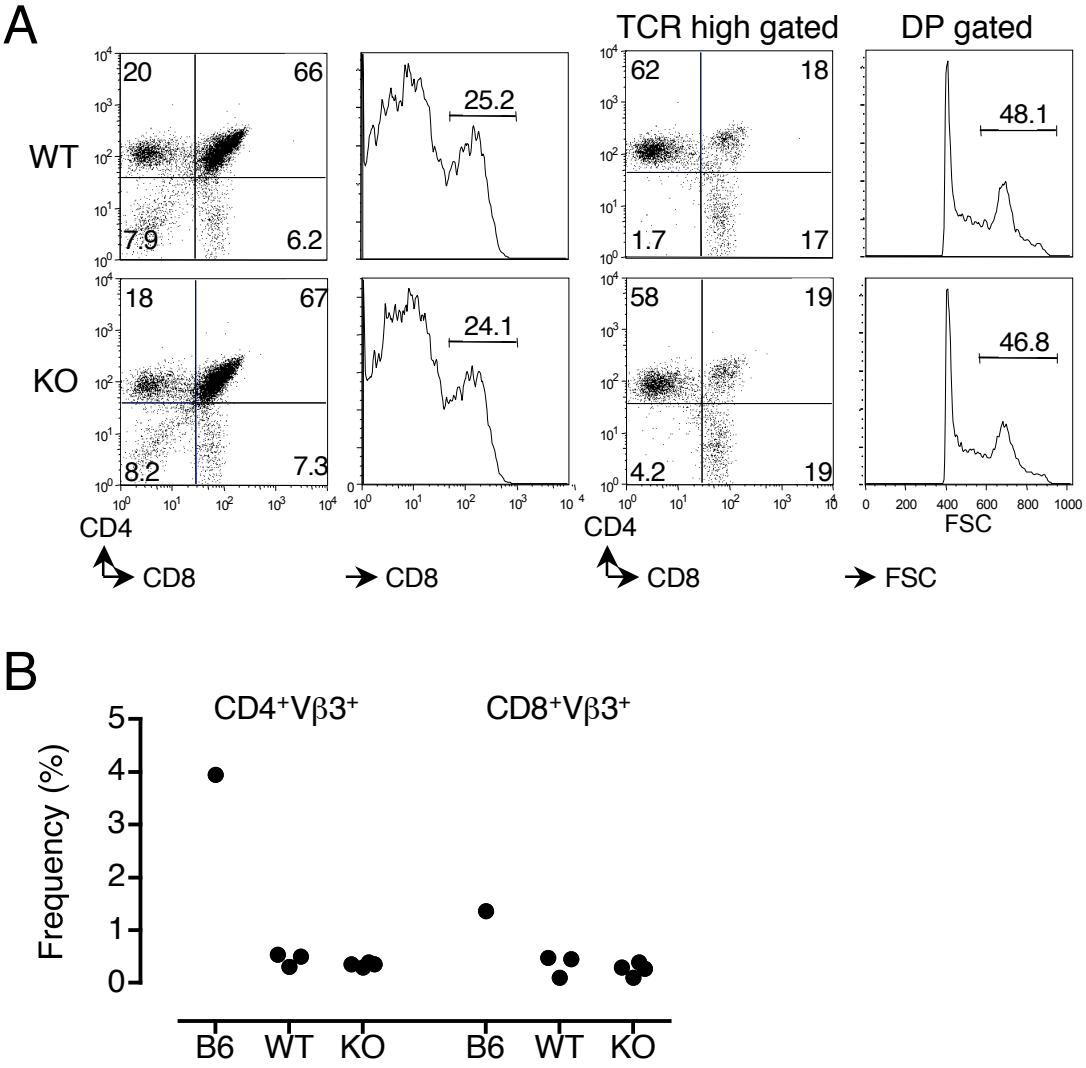

Supplemental Figure 2: Normal thymic selection of polyclonal αβ T cell in Tssp° NOD mice

(A) Thymocytes were analyzed for expression of CD4, CD8α and TCR β chain. The CD4/CD8 distribution is shown without and with electronic gating on αβTCR^{high} (i.e. post-selection) thymocytes. The right panel shows the FSC profile of CD4$^+$CD8$^+$ double positive immature thymocytes and the percentage of FSC high cells, corresponding to immature CD4$^+$CD8$^+$ T cells undergoing positive selection, is indicated. (B) The deletion of Vβ3$^+$ T cells imposed by the *mtv-3* encoded superantigen was as efficient in Tssp° NOD mice and WT control mice. Frequency of Vβ3 expressing cells among CD4 (left) and CD8 (right) T cells from Tssp° (KO) and control (WT) NOD mice. A C57BL/6 mouse (B6) was used as control for Vβ3$^+$ cell frequency observed in the absence of *mtv-3* encoded superantigen. Each symbol represent an individual mouse.

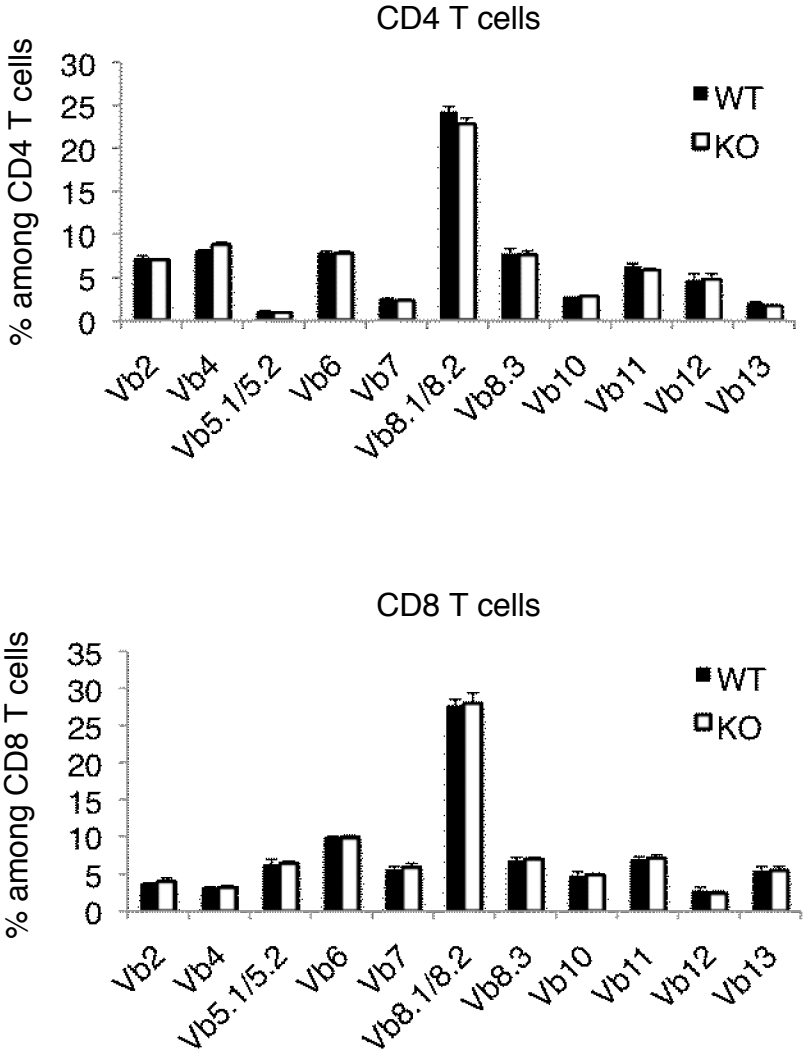

Suppplemental Figure 3: Vbeta segment usage by peripheral CD4 and CD8 T cells from Tssp° and control NOD mice.

LN cells from Tssp° (KO) and control (WT) NOD mice were stained for CD4, CD8 and Vbeta expression prior to analysis by flow cytometry. The Vbeta usage is represented as the percentage of positive cells after electronic gating on CD4 (Top panel) and CD8 (Bottom panel) T cells. Data represent the mean ± SD of 4 individual mice for each genotype analyzed in 2 separate experiments.

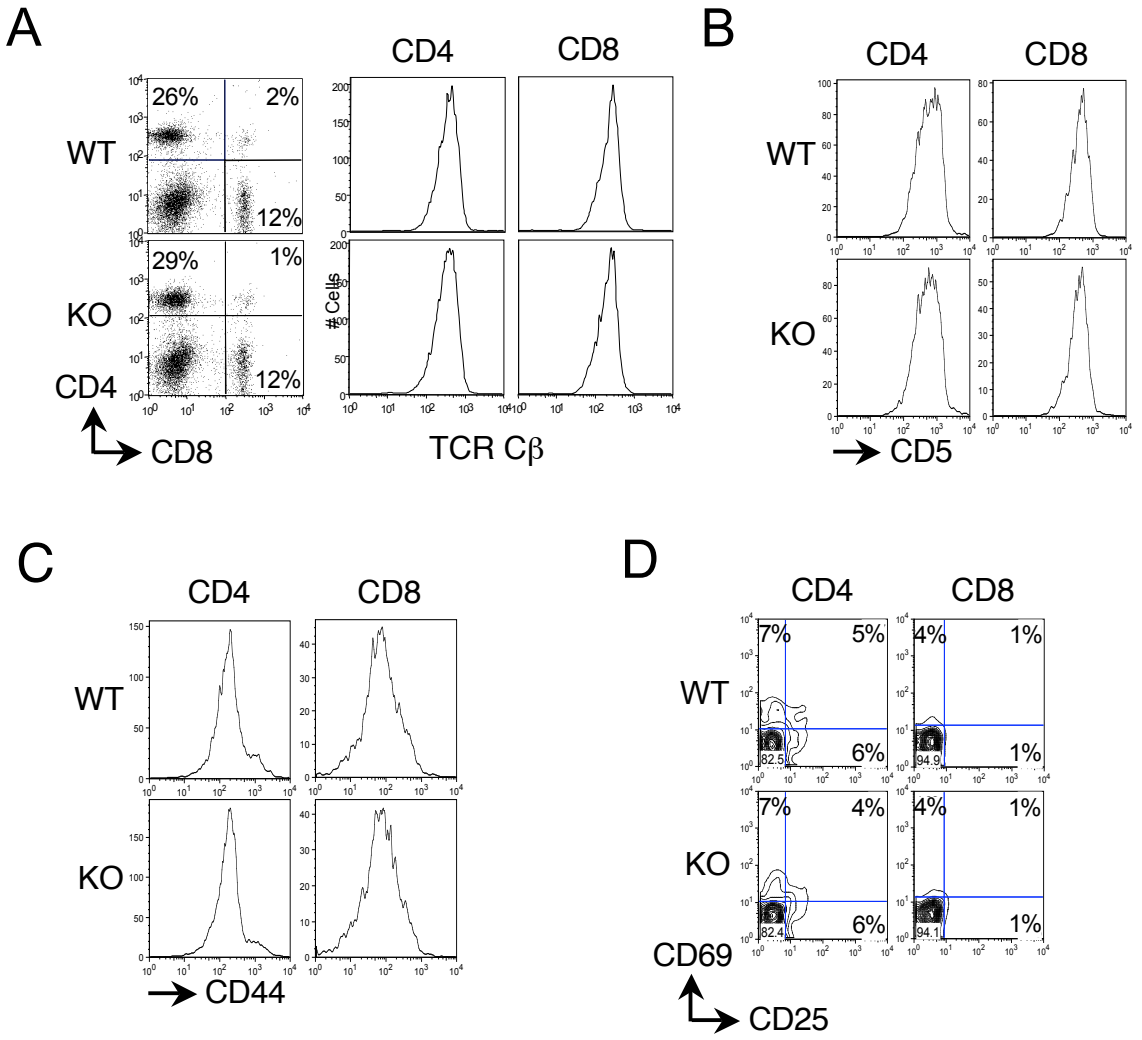

Supplemental Figure 4: Phenotypic features of peripheral CD4 and CD8 T cells from Tssp° and control NOD mice.

LN cells of unprimed WT or Tssp° (KO) NOD mice were analyzed by multi-color staining for surface expression of CD4, CD8α and TCRβ (**A**). The CD5 (**B**) and CD44 (**C**) expression profiles are shown for CD4 or CD8 T cells. (**D**) CD25 and CD69 expression by CD4 and CD8 T cells are represented as contour-plots. Percentages of cells within each quadrant are indicated. Similar profiles were observed for splenic T cell subsets (not shown).

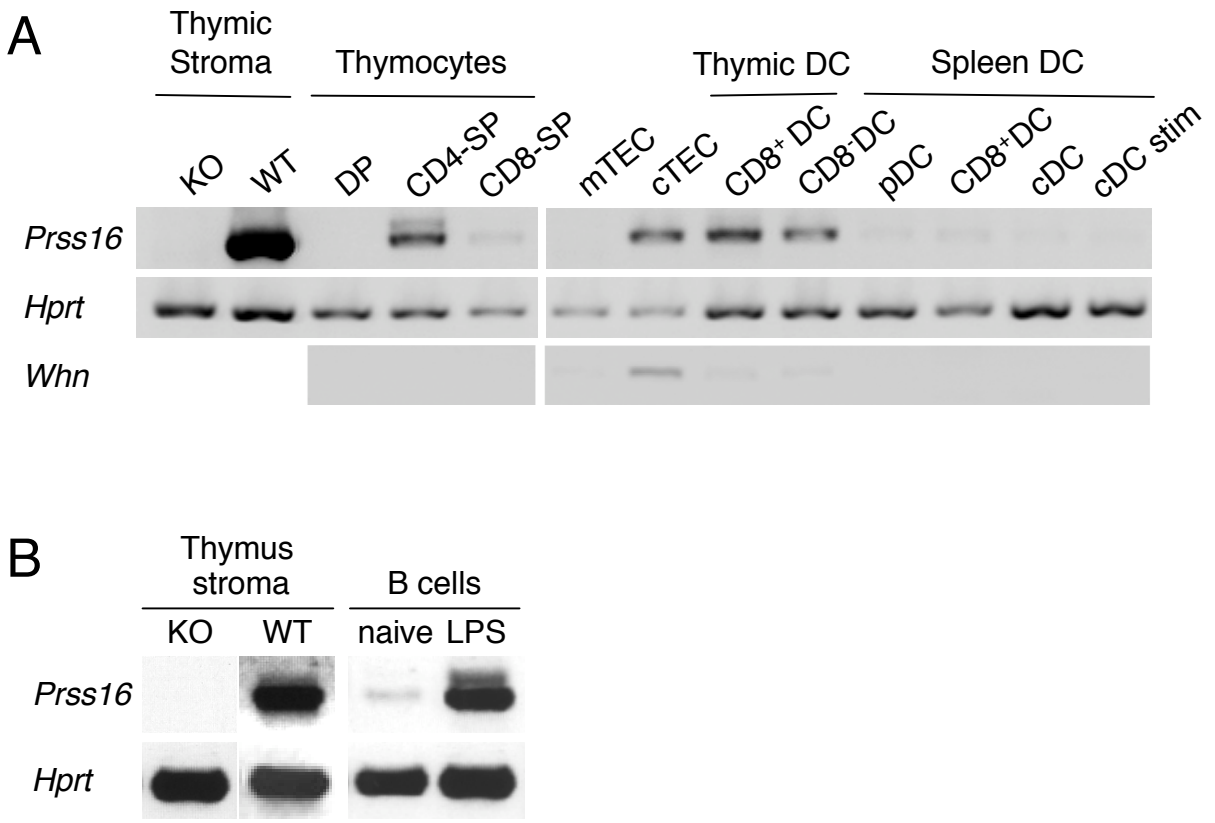

Supplemental Figure 5: Tssp expression pattern in the thymus and peripheral B cells and dendritic cells.

Total RNA was extracted from the indicated tissues. The thymic stroma of Tssp° (KO) and control (WT) NOD mice refer to the tissue remaining after mechanical elimination of thymocytes. Other cell subpopulations were isolated from WT NOD mice as described in the supplemental method section. Spleen cDC correspond to $CD11c^{+}CD8^{-}B220^{-}$ DC that were left unstimulated or stimulated (cDC stim) with 2.5ng/ml polyIC and 10μg/ml LPS. Spleen B cells were stimulated or not (naive) with 10μg/ml LPS for 2 days (LPS). The specificity of the reaction is demonstrated by the absence of amplification in thymic stroma of Tssp° thymus or hematopoietic cells of Tssp° NOD mice (not shown). (**A**) 100ng of stromal ARN, or 10^4 purified cells were used for the RT-PCR reaction except for mTEC and cTEC where 5000 cells were used. *Whn* is a cTEC specific transcript and serves as control for cTEC contamination in other thymic subpopulations. (**B**) Same as in (**A**) except that 10^5 B cells were used. (**A**) and (**B**) are from 2 independent experiments. *Hprt* was used as endogenous gene control. Similar results were obtained in 2 independent experiments.

A

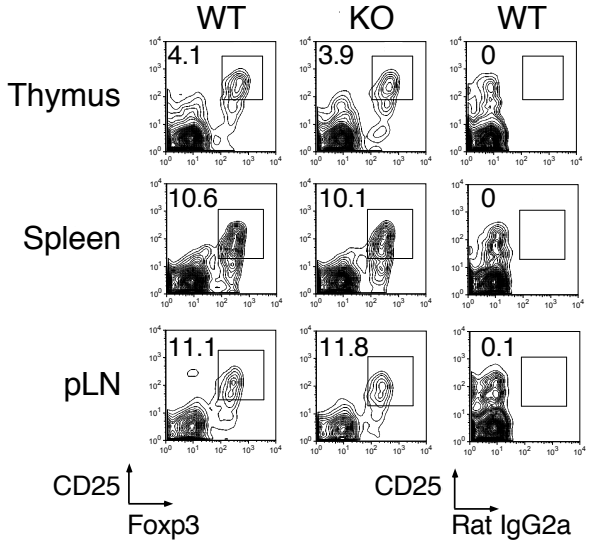

B

		% CD25^{hi}Foxp3^{+} among CD4 T cells*	Number CD25^{hi}Foxp3^{+} among CD4 T cells (10^6)
Thymus	WT (n=9)	6.99 ± 1.1	1.96 ± 1.4
	KO (n=10)	7.24 ± 1.7	2.21 ± 0.7
Spleen	WT (n=9)	9.95 ± 1.9	2.49 ± 0.36
	KO (n=10)	10.05 ± 1.5	2.57 ± 0.6
pLN	WT (n=7)	9.37 ± 2.6	0.93 ± 0.02
	KO (n=7)	9.59 ± 2.9	0.94 ± 0.04

Supplemental Figure 6: Representation of CD25^{hi}Foxp3^{+}CD4^{+} T cells in lymphoid organs of Tssp° and WT NOD mice.

(**A**) Foxp3 versus CD25 profile of gated CD4 T cells from Tssp° and WT NOD mice. Cell suspensions were FACS-analyzed after CD4/CD8/CD25/Foxp3 staining. The values represent the percentage of CD25^{hi}Foxp3^{+} cells among either CD4-SP thymocytes or CD4 T cells from spleen and pancreatic lymph nodes (pLN). An isotype control staining is shown for a WT mouse (right part of the panel).

(**B**) The values represent the mean ± SD frequency and the absolute number of CD25^{hi}Foxp3^{+} CD4^{+} T cells in the thymus, spleen and pLN of Tssp° (KO) and WT control NOD mice. The percentage were derived according to the gating strategy indicated in (A). The absolute numbers were calculated by combining the relative frequency of the CD25^{hi}Foxp3^{+}CD4^{+} T cell subset and the absolute number of CD4 T cells for each organ. The n value corresponds to the number of mice analyzed. None of the differences observed were statistically significant. * In the case of the thymus, "CD4 T cells" refers to the CD4-SP subset of thymocytes.

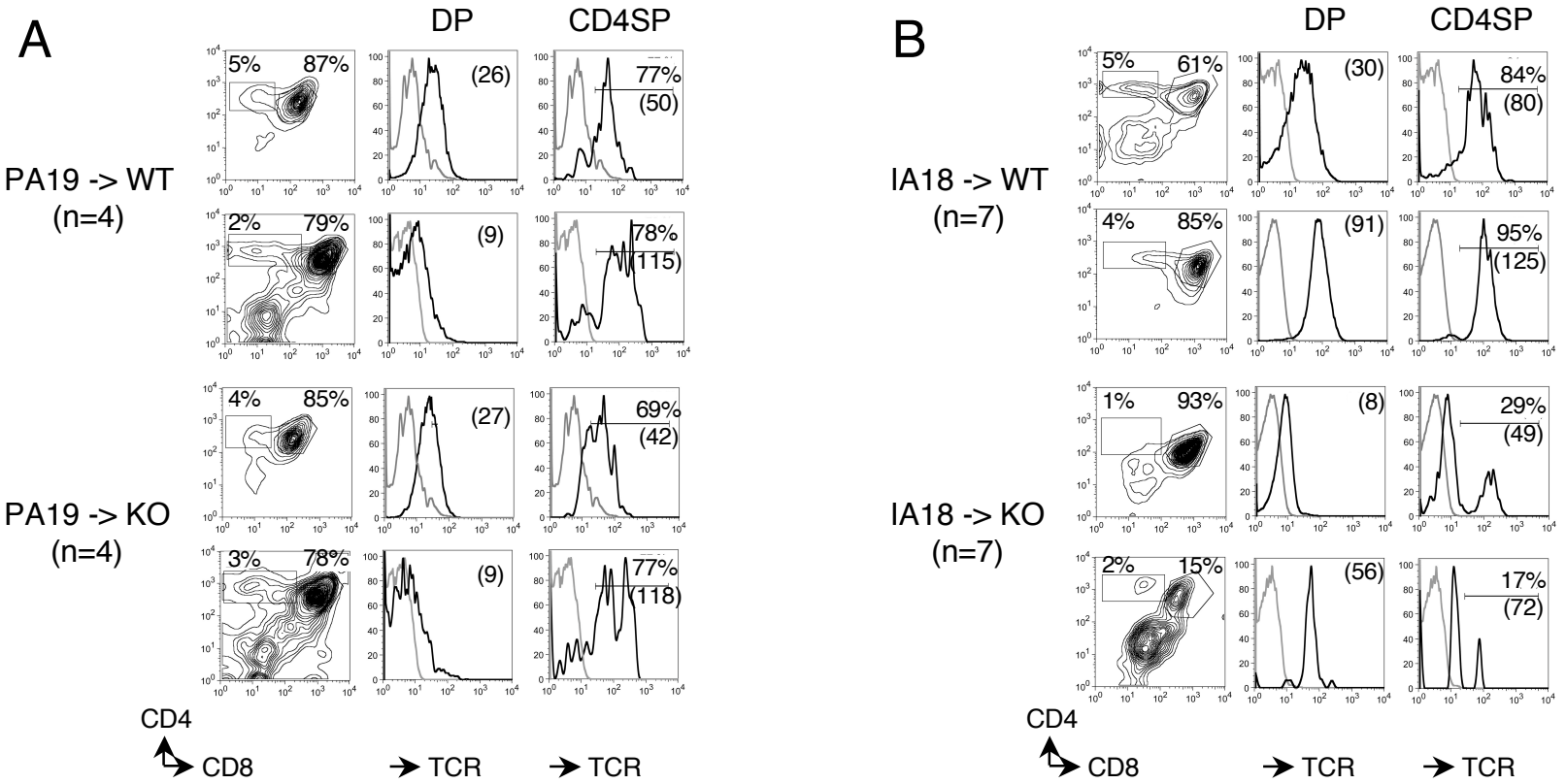

Supplemental Figure 7: Additional FACS profiles showing the phenotype of retrogenic thymocytes expressing the islet antigen-specific PA19 and IA18 TCR.

The representation of the data is identical to that depicted in Figure 7. Briefly, the CD4/CD8 distribution of EGFP$^+$ total thymocytes and the TCR profile of electronically gated DP and CD4-SP thymocytes are shown. The percentage and, in parenthesis, the TCR MFI of TCR$^+$ DP and CD4-SP thymocytes are shown in the upper part of the relevant histogram. Shaded histograms correspond to unstained controls. The profiles of two individual mice are displayed per group. **(A)** PA19 TCR. **(B)** IA18 TCR.

Supplemental Methods

Mice

B6-*Prss16*$^{-/-}$ mice have been described previously (1). To generate Tssp-deficient (Tssp°) NOD mice along with WT controls, *Prss16*$^{-/-}$ mice on a mixed C57BL/6x129/sv background were backcrossed onto the NOD/LtJ background. At the second backcross generation, *Prss16*$^{+/-}$ mice homozygotes for the NOD I-A^{g7} class II allele were selected for further backcrossing for up to 13 generations and heterozygous mice were intercrossed at the 6-, 10 and 13-backcross generation. At the N6 backcross generation, microsatellites analysis showed that the genetic regions related to most known *idd* loci were of the NOD background. Notably, *Idd*1, *Idd*3, *Idd*5, *Idd*10, *Idd*16, *Idd*18 and *Idd*23, the *idd* loci reported to have a significant impact on insulitis and diabetes (2), and *Idd*14, the only *Idd* locus on chromosome 13, were of the NOD background (Supplemental Figure 1A). At the 10 and 13-backcross onto NOD, all known *idd* loci were of NOD origin (Supplemental Figure 1B). Using available polymorphism markers we showed that at the N13 generation, the genetic makeup is of NOD origin starting at least at 1cM proximal and 12cM distal of *Prss16* (Supplemental Figure 1B). Importantly, congenic NOD.B6*Idd*14 mice that carry the B6-derived genetic interval from 13cM-71cM (*prss16* is at 10cM) show increased diabetes susceptibility as compared to NOD mice indicating that in B6 mice this interval does not include diabetes resistance, but instead a diabetes susceptibility loci (3). In addition, genome wide analysis of diabetes susceptibility loci excluded a significant contribution of region on chromosome 13, beside *Idd*14, to diabetes or insulitis (4).

Tssp-deficient NOD scid mice and NOD scid control were generated by intercrossing heterozygous N10F1 NOD mice with NOD/SCID. Similarly Tssp-deficient NOD-Ca° mice and NOD-Ca° control were generated by intercrossing heterozygous N13F1 NOD mice with NOD-Ca°.

Microsatellite analysis

Microsatellite analysis was performed on genomic DNA from Tssp° and control WT NOD mice by using genetic markers related to regions containing all known *idds*. Primer sequences allowing for distinction between C57BL/6, 129/Sv and NOD alleles were obtained from Mouse Genome Informatics database (www.informatics.jax.org)..

MAbs and flow cytometry

Cells were stained with a combination of FITC-, PE-, APC-, and PerCP-Cy5.5-conjugated Abs. MAbs to CD4 (clone RM4-5), CD8 (53-6.7), B220 (RA3-6B2), TCRCβ (H57-597), Vβ3 (KJ25), CD25 (PC61.5), CD69 (H1.2F3), and Thy1.1 (OX-7), CD44 (IM7), CD5 (53-7.3), CD62L (Mel14) were obtained from eBioscience or BD Biosciences. TCR Vβ distribution among CD4 and CD8 splenic T cells was analyzed by three-color staining with a Vβ TCR Screening Panel (BD Biosciences).

RNA preparation and RT-PCR

B cells were prepared by negative selection as described in the Methods section of the main manuscript. Thymocytes subpopulations were FACS sorted based on CD4 and CD8 expression. For DC isolation, spleen and thymus of at least 10 NOD mice were digested with Liberase (Roche) and DNase (Sigma) prior to positive selection with anti-CD11c magnetic beads (Miltenyi Biotech). The pre-enriched thymic DC preparation was stained with anti-CD45.1-PE, anti-CD11c-APC and anti-CD8-Pacific blue Abs and $CD45.1^+$ $CD11c^+CD8^+$ ($CD8^+$ DC) and $CD45.1^+CD11c^+CD8^-$ ($CD8^-$DC) cells were FACS-sorted. The pre-enriched spleen DC preparation was stained with anti-CD11c-APC, B220-FITC and CD8-Pacific Blue Abs and sequential gating strategy was applied to FACS-sort $CD11c^{int}B220^+$ (pDC); $CD11c^+CD8^+B220^-$ ($CD8^+$DC) and $CD11c^+CD8^-B220^-$ (cDC) cells. To isolate cTEC and mTEC population, thymi were digested with Liberase and DNase and supernatant was removed after 10min sedimentation at 1g. The pellet corresponding to stromal tissue was further digested with Liberase, Dispase I (Roche) and DNase. The recovered cell population was depleted of hematopoietic cells using anti-CD45.1-PE antibodies and anti-PE magnetic beads (Miltenyi Biotech) and stromal cells were FACS-sorted following staining with biotin-conjugated anti-BP1, APC-conjugated anti-mouse EpCAM and Pacific blue-conjugated Streptavidin. Total RNA was extracted using the High Pure RNA Isolation kit (Qiagen) and cDNA was synthetized using random primers as previously described (5). The PCR reaction was performed on cDNA using the GoTaq® DNA Polymerase (Promega). The primer sequences for the *Prss16* coding sequence are forward: 5'-TGCGCAGCATGGGACAGAAG-3' and reverse: 5'-AGTCTGAAGGCCTCATAGGTG-3', for *Whn* are forward: 5'-ACACCAGCAGCCATTGTTCC-3' and reverse: 5'-CCAAGCTGTCATCCTTCAGC-3' and for *Hprt* are forward: 5'-GTTGGATACAGGCCAGACTTTGTTG-3' and reverse: 5'-GAGGGTAGGCTGGCCTATGGCT-3'.

Peptide sequences

The peptide were produced by Genecust (Luxemburg) and designed based on published sequences (6, 7). The peptide sequences are: Ins_{9-23} : SHLVEALYLVCGERG; Ins_{49-66} : GAGDLQTLALEVAQQKRG; $GAD_{206-220}$: TYEIAPVFVLLEYVT ; $GAD_{524-543}$: SRLSKVAPVIKARMMEYGTT ; $IGRP_{4-22}$: LHRSGVLIIHHLQEDYRTY ; $IGRP_{132-145}$: WYVMVTAALSYTISRMEESSVTL ; $IGRP_{195-214}$: HTPGVHMASLSVYLKTNVFL ; IA-$2\beta_{755-777}$: REENAPKNRSLAVLTYDHASRI ; $HA_{512-520}$: LAIYATVAG

Supplemental References

1. Gommeaux, J., Gregoire, C., Nguessan, P., Richelme, M., Malissen, M., Guerder, S., Malissen, B., and Carrier, A. 2009. Thymus-specific serine protease regulates positive selection of a subset of CD4(+) thymocytes. *Eur J Immunol* 39:956-964.
2. Todd, J.A., and Wicker, L.S. 2001. Genetic protection from the inflammatory disease type 1 diabetes in humans and animal models. *Immunity* 15:387-395.
3. Brodnicki, T.C., Quirk, F., and Morahan, G. 2003. A mouse Susceptibility Allele From a Non-Diabetes-Prone Mouse Strain Accelerates Diabetes in NOD Congenic Mice *Diabetes* 52:218-222.
4. Ghosh, S., Palmer, S.M., Rodrigues, N.R., Cordell, H.J., Herane, C.M., Cornall, R.J., Prins, J.-B., McShane, P., Lathrop, G.M., Peterson, L.B., et al. 1993. Polygenic control of autoimmune diabetes in nonobese diabetic mice. *Nat Genet* 4:404-409.
5. Bajenoff, M., Wurtz, O., and Guerder, S. 2002. Repeated antigen exposure is necessary for the differentiation, but not the initial proliferation, of naive CD4(+) T cells. *J Immunol* 168:1723-1729.
6. Lieberman, S.M., and DiLorenzo, T.P. 2003. A comprehensive guide to antibody and T-cell responses in type 1 diabetes. *Tissue Antigens* 62:359-377.
7. Mukherjee, R., Wagar, D., Stephens, T.A., Lee-Chan, E., and Singh, B. 2005. Identification of CD4+ T cell-specific epitopes of islet-specific glucose-6-phosphatase catalytic subunit-related protein: a novel beta cell autoantigen in type 1 diabetes. *J Immunol* 174:5306-5315.